*Concept Paper*

# Climate-Quality Calibration for Low Earth-Orbit Microwave Radiometry †

**Philip W. Rosenkranz** [1,*,‡] **William J. Blackwell** [2] **and R. Vincent Leslie** [2]

1   Massachusetts Institute of Technology, Cambridge, MA 02139, USA
2   MIT Lincoln Laboratory, Lexington, MA 02420, USA; wjb@ll.mit.edu (W.J.B.); lesliev@ll.mit.edu (R.V.L.)
*   Correspondence: phil.rosenkranz@alum.mit.edu
†   This paper is an extended version of our paper published in the 2019 Joint Satellite Conference, Boston, MA.
‡   Retired.

**Abstract:** Improvements in radiometric calibration are needed to achieve the desired accuracy and stability of satellite-based microwave-radiometer observations intended for the production of climate data records. Linearity, stability and traceability of measurements to an SI-unit standard should be emphasized. We suggest radiometer design approaches to achieve these objectives in a microwave calibration-reference instrument. Multi-year stability would be verified by comparison to radio-occultation measurements. Data from such an instrument could be used for climate studies and also to transfer its calibration to weather-satellite instruments. With the suitable selection of an orbit, a climatology of the diurnal variation in the measured parameters could be compiled, which would reduce uncertainties in climate trends inferred from earlier microwave radiometers over past decades.

**Keywords:** microwave radiometer calibration; GSICS; intercalibration

## 1. Introduction

Accuracy and long-term consistency in space-based measurements of the earth require comparisons of satellite instruments to one another and to high-accuracy reference instruments [1]. For these calibration intercomparisons to be useful for climate studies, they must be traceable to standards that are stable over decades, in order to exclude the possibility of measurement drifts that would obscure long-term atmospheric trends. The proposed CLARREO mission [2,3] would provide reference-standard measurements at infrared and visible wavelengths. In the microwave part of the spectrum, improvements have been made with each new generation of weather-satellite instruments, but as yet, no single instrument combines all of the features of a calibration system that would constitute a state-of-the-art calibration standard.

Although microwave sounding instruments on weather satellites have been used to monitor global trends in atmospheric temperature (see the discussion in [4]), they were designed to observe weather phenomena. The requirements for the two types of measurement are different. Weather observations benefit from good spatial resolution (i.e., narrow antenna beams) and radiometric resolution (i.e., low noise) because individual measurements are assimilated into a numerical prediction model. For monitoring of climate, the measurements are spatially averaged and temporally smoothed, so calibration-related issues predominate in the error budget. For example, any non-linearity in radiometer response introduces scene-dependent errors with adverse consequences for the determination of long-term trends [5]. Therefore, a microwave radiometer designed as a reference instrument in a space-based climate observing system would differ in several respects from weather-satellite instruments. The antenna should have extremely low sidelobe levels; there is no trade-off with respect to a narrow beamwidth requirement as in the case of weather satellites.

The radiometer should have excellent linearity and stability in both frequency and calibration accuracy, with on-orbit traceability in SI units.

In this paper we focus on orbital radiometric calibration in the 50–60 GHz frequency band for long-term temperature monitoring. However, most of the features discussed in Section 2 would facilitate inter-satellite transfer-calibration at frequencies used by microwave imagers as well as sounders. Section 3 discusses occultation of Global Navigation Satellite System (GNSS) signals as a comparison reference to provide traceability of radiometer stability to frequency standards. Other sources for comparisons are radiosondes, ground-based radiometers, and vicarious calibration scenes [6–8]. Section 4 considers some factors relevant to the choice of an orbit for a reference satellite.

Pre-launch calibration of target emissivity and temperature sensors, although an essential part of an instrument calibration plan, is not within the scope of this paper. However, a recent development in that area at the U.S. National Institute of Standards and Technology is described in [9].

## 2. Radiometer Design

Rather than prescribing a detailed instrument design here, we recommend some approaches to achieve accuracy, linearity, stability, and SI-traceability. The following design features [10,11] would be desirable in a microwave reference radiometer:

- A phase-locked local oscillator (LO) prevents frequency drift.
- The system response of the amplifiers and detectors should be as nearly as possible linear with input power. An internal noise diode will allow correction of residual non-linearity. Firing the noise diode during part of the viewing time of high and low calibration temperatures yields four calibration points, which can be solved for three coefficients of the instrument transfer function (e.g., a quadratic form) and also the excess noise temperature of the diode [12]. (The noise temperature of the diode is not assumed to be constant.) However, nonlinearity in common amplifier stages can introduce crosstalk between channels because of gain compression [13], which this method will not correct. Therefore, linearity is extremely important for those amplifiers. Digital processing may be useful in this context, given that the non-linearity inherent in binary representation of signals can be corrected analytically [14].
- Instead of total power detection, sensitivity to short-term gain fluctuations within the calibration cycle should be reduced by Dicke-switching, by digital correlation, or by some other means.
- A low-sidelobe horn antenna without a reflector eliminates spillover of energy at the edge of the reflector, making the directivity pattern accurately calculable. The radiometer section would rotate along with the antenna, to scan the earth and also view cold space and an on-board black-body target, as sketched in Figure 1. A monostatic return loss of 55 dB from 31 to 84 GHz has been measured on a folded inverted-cone target [15]. The antenna should be closely coupled to the target when viewing it.
- The scan should include the earth limbs for comparison of limb radiometric measurements to GNSS radio-occultation (RO) measurements, as discussed below in Section 3. Comparison with radiometric measurements at the limb instead of closer to nadir avoids the difficulties associated with different viewing geometries (e.g., see [16]).
- Dual-polarization measurements, using two radiometers coupled to orthogonal modes of the antenna, allow exact transfer of calibration to rotating-polarization instruments like ATMS, for channels sensitive to surface polarization. For frequencies not sensitive to the surface, the two polarization measurements would be averaged together.
- Control of instrument temperature, including the calibration target, contributes to radiometer stability and also simplifies requirements for pre-launch testing.
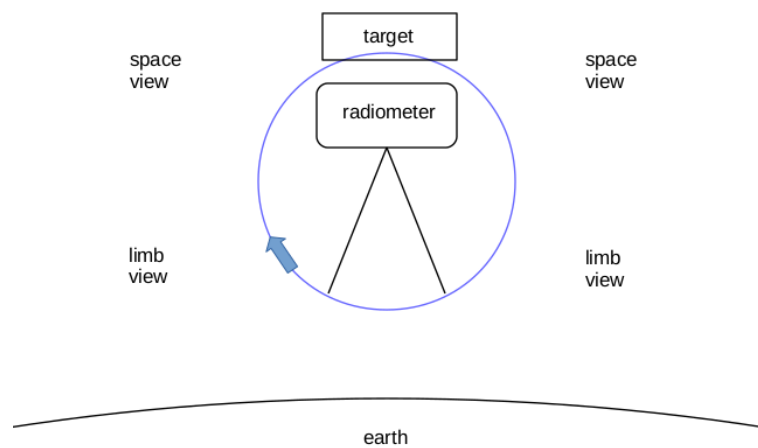
**Figure 1.** Radiometer/antenna/target scanning configuration.

In addition to monitoring climate trends, an orbiting microwave reference radiometer designed in this way could transfer its calibration accuracy to weather-satellite instruments, whose data are assimilated into forecast models. Several footprints of the other instrument can be combined in that comparison, so the reference-radiometer's antenna beamwidth can be as large as several degrees. To serve as a calibration reference for sounders like ATMS or SSMIS, the reference instrument may need to duplicate only a few channels for each target on the other radiometer (assuming that target emissivity is a smooth function of frequency). The MSU channel frequencies would also be among those with a high priority, but for the purpose of providing long-term continuity of climate measurements.

In the 50–60 GHz band, the instrument characteristics listed in Table 1 should be achievable with currently available technology. The first four are k = 1 uncertainties, while the others should be interpreted as upper limits. Radiometer noise for a 400 MHz passband is 0.05 K at 1 s integration, but the actual integration time $\tau_r$ will depend on the scan rate.

**Table 1.** Characteristics of a calibration-reference radiometer for 50–60 GHz.

| Parameter | Value | Comments |
|---|---|---|
| (noise-equivalent $\Delta T$) $\cdot \tau_r^{1/2}$ | $\leq$0.05 K s$^{1/2}$ | for dual-polarization average |
| absolute accuracy of calibration at launch | $\pm$0.1 K | for antenna temperature |
| (long-term calibration stability $\delta T_A$) $\cdot (\Delta t)^{1/2}$ | $\pm$0.01 K yr$^{1/2}$ | Equation (3), with GNSS-RO reference |
| lifetime frequency stability | $\pm$1 MHz | with phase-locked LO |
| antenna 3 dB beamwidth | 5° | from [11] |
| antenna stray factor (1 – beam-efficiency) | $\leq$1% | >15° from beam center |
| antenna off-earth stray factor | $\leq$0.03% | for nadir view |
| non-linearity max. deviation (before correction) | $\leq$0.1 K | for $3 \leq T_A \leq 300$ K |

## 3. Co-Located Radio-Occultation Reference

The radiometer would be accompanied by a GNSS-RO receiver and antenna, to enable referencing of limb measurements to microwave brightness temperatures inferred from simultaneous radio-occultation measurements of refractivity at the same elevation and azimuth angles [11]. This achieves similar horizontal averaging along the path through the atmosphere, as illustrated by Figure 2. (Elevation is equivalent to scan angle, and azimuthal alignment of the radiometer beam with the GNSS signal could be achieved either by adjustment of spacecraft yaw, or with a gimbal mount for the radiometer, see for example [17]). Occultations that occur close to the plane of the orbit are the most desirable, because a satellite in a low earth orbit moves faster than a GNSS satellite. These comparisons will track long-term stability of the target's emissivity and temperature sensors, and also provide another way to monitor possible scene-dependent error over time, because limb brightness temperature varies with angle over a wide range.
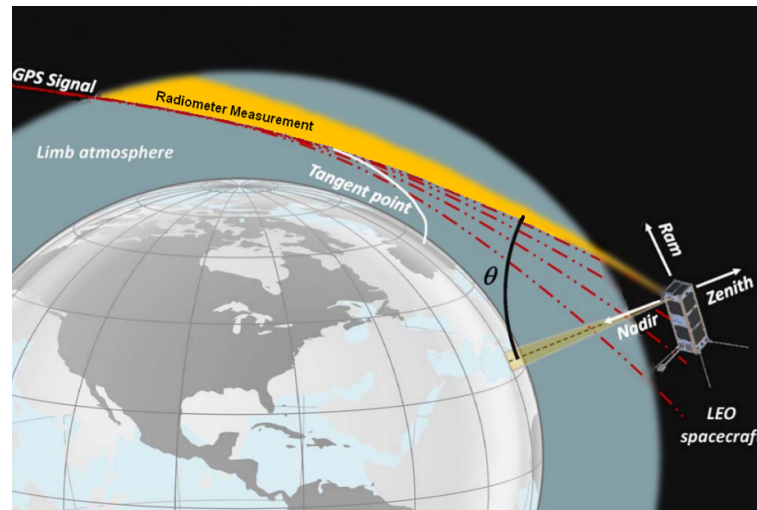
**Figure 2.** Basic geometry of co-located GNSS-RO microwave radiometer calibration [11].

The underlying observable in RO is the additional Doppler shift of the GNSS signal relative to that which would be observed in the absence of an atmosphere [18]. That Doppler shift is the time-derivative of phase delay due to refractive index along the atmospheric path, and it can be accurately measured [19,20]. Thus, the RO atmospheric refractivity profile is ultimately traceable to a frequency standard. Radiometer comparisons with occulted GNSS signals would depend on the microwave transmittance model used to calculate brightness temperature and on the atmospheric refractivity retrieval. Uncertainties in microwave spectroscopic parameters have been reviewed, and their influence on calculated brightness temperature quantified, in [21].

The refractive index *n* of the clear atmosphere can be modeled as

$$n - 1 = k_1 \rho_f + (k_2 + k_3/T)\rho_w + k_4 \rho_c, \tag{1}$$

where $\rho_f, \rho_w$ and $\rho_c$ are the number densities of fixed-abundance gases, water vapor, and carbon dioxide respectively, and $T$ is Kelvin temperature. A recent review of published measurements of the coefficients $k_1, k_2, k_3$ and $k_4$ is given in [22]. There is some dispersion within the oxygen band, but the microwave value of $(n - 1)$ would be within a few percent of its value for the lower frequencies of the GNSS signals. Hence a microwave ray through the limb atmosphere would closely approximate the GNSS signal path. The main difference is that the radiometer measures brightness temperature integrated over the antenna's directivity pattern.

In the stratosphere, where the atmosphere is very dry, the hydrostatic equation can be used to unambiguously relate refractivity to the profiles of temperature and pressure vs. height [18], which determine the limb brightness temperature by means of the transmittance model. The lower troposphere generally contains more moisture, which varies independently of temperature. Consequently, these comparisons would be useful for channels in an $O_2$-band but less so for water or window channels. Oxygen-band weighting functions that peak in the troposphere for a near-nadir view angle will move into the stratosphere at limb-viewing angles. Hence a full channel set can be compared at the limb with RO measurements, whereas comparisons of tropospheric channels near nadir would require ancillary knowledge of humidity. Surface emissivity also ceases to be a significant factor at the limb.

Due to its dependence on both microwave transmittance model and refractivity retrieval, it is unlikely that the RO reference would improve on the absolute accuracy of on-board calibration with the target and cold space (at least at launch), but if the computer algorithms are applied in a uniform way to a time series of measurements [23], then RO provides a stable reference to determine whether the on-board target's calibration is also stable. Although no physical mechanism causing changes in target components has been identified, their long-term stability in the space environment cannot be verified

without reference to an independent standard. Ideally, GNSS-RO comparisons would verify that the on-board calibration is stable over many years; and indeed, over a 14-year time span, stratospheric AMSU channels on the Aqua satellite closely tracked RO temperature retrievals [24]. (The stratospheric channels of AMSU have a phase-locked local oscillator.) But if such comparisons diverge over an instrument's lifetime, the trend derived from the radiometer could be adjusted accordingly.

The "long-term stability" in Table 1 is derived from the variance of uncertainty in determination of the trend $m$ in a time series over an interval $\Delta t$ [25].

$$\langle(\delta m)^2\rangle = 12(\Delta t)^{-3}\sum_i \sigma_i{}^2 \tau_i, \tag{2}$$

in which the summation is over independent sources of error with variances $\sigma_i{}^2$ and autocorrelation time constants $\tau_i$. Here we consider only the contribution of the variance associated with the radiometer-to-RO comparison. In other words, any bias due to the transmittance and refraction models does not affect the precision of the comparison. Also, we do not distinguish here between a trend due to climate change and a trend due to shorter-term atmospheric variability over the interval $\Delta t$. Replacing $\delta m$ with $\delta T_A / \Delta t$, where $\delta T_A$ is the uncertainty in the calibration adjustment from the RO comparisons, gives

$$\langle(\delta T_A)^2\rangle \Delta t = 12\sigma^2 \tau. \tag{3}$$

Simulations of radiometer calibration in the 50-60 GHz band with RO [11] show rms uncertainty of 0.1 to 0.25 K, depending on how well antenna pointing is known. Considering random errors to be uncorrelated between occultations, $\tau$ will be the average time between occultations. We assume 4000 occultations per year to be selected from >60,000 potential occultations for one receiving satellite (this degree of selectivity might not require any azimuthal steering of the radiometer beam). Then setting $\sigma = 0.2$ K yields $(\delta T_A)_{rms} = 0.01$ K in one year, or 0.003 K in a decade. For a constant rate of occultations, $(\delta T_A)_{rms}$ decreases with the square root of the time interval, in analogy with the behavior of integrated radiometer noise.

Because of the traceability of their measurements to frequency standards, changes of GNSS-RO instruments do not introduce offsets in a long-term record [20]. Thus, for the purpose of creating a multi-decadal climate record during which replacement of reference-radiometer satellites is necessary, inter-radiometer calibration offsets would be removed by double-differencing with the RO reference. Overlap of reference microwave radiometers' lifetimes would be less important and probably not even necessary. Using the RO reference in this way avoids the accumulation of error variances in a chain of radiometer calibration transfers by single-differencing, which would introduce an uncertainty in the inferred multi-decadal trend.

## 4. Orbit Selection

The orbit should facilitate inter-satellite calibration of instruments on several weather satellites. A 90º-inclination orbit would intersect weather-satellite orbits at a distribution of latitudes [3]. Also, that orbit would not precess in sidereal time, so the measurements would cycle through local solar time and seasonal cycles (see Table 1 in [2]), unlike the very slow drift in equator-crossing time which created problems with the measurements from some weather satellites [26]. Hence it would provide a truer global average than a sun-synchronous orbit.

A further benefit of a non-sun-synchronous orbit would be the possibilty of modeling the climatology of the diurnal and seasonal cycles of temperature, as a function of location. Better knowledge of the diurnal cycle could reduce uncertainties in the trends of tropospheric temperature inferred from MSU measurements starting from 1979. For example, one can calculate from Table 2 in [26] that 75% of the total variance of uncertainty in the global lower-troposphere temperature trend for the period 1979–2009 is due to the diurnal adjustment (which in that case was obtained from a general-circulation model). In subsequent work [27,28] a second-harmonic correction to

the model-simulated diurnal adjustment was derived from the satellite measurements, yielding improved agreement of trends from different satellite radiometers. This suggests that the availability of non-sun-synchronous satellite measurements might also stimulate improvements to the treatment of atmospheric energy flow in general-circulation models (which now can be tested only against sun-synchronous satellite measurements and twice-daily radiosonde launches), thus leading to better representation of the diurnal cycle in the models.

Finally, it is desirable for the spacecraft to use propulsion to maintain orbit altitude, because altitude decay changes the relation of scan angle to earth incidence angle [29].

## 5. Summary and Conclusions

Monitoring of long-term atmospheric trends, especially of temperature, requires radiometric stability and linearity, whereas radiometric resolution and spatial resolution become less important than for weather observations. We have described how radiometer design could be optimized for the former purpose, and it differs in some respects from the design of existing weather-satellite instruments. By referencing to radio-occultation measurements, radiometer stability would be traceable to frequency standards. By means of the limb-view RO comparisons, all channels, including those with lower-troposphere weighting functions at nadir, would acquire this stability. A suitable selection of orbit would permit derivation of a climatology of the diurnal cycle of temperature, with benefits for the interpretation of trends from weather-satellite radiometers over the past four decades. Further evaluation of radiometer configurations, target design, scan pattern, orbit, and error analysis would be warranted.

## Abbreviations

The following abbreviations are used in this manuscript:

| | |
|---|---|
| AMSU | Advanced Microwave Sounding Unit |
| ATMS | Advanced Technology Microwave Sounder |
| GNSS | Global Navigation Satellite System |
| LO | local oscillator |
| MSU | Microwave Sounding Unit |
| RO | radio occultation |
| SSMIS | Special Sensor Microwave Imager/Sounder |
| $T_A$ | antenna temperature |

## References

1. Goldberg, M.; Ohring, G.; Butler, J.; Cao, C.; Datla, R.; Doelling, D.; Gärtner, V.; Hewison, T.; Iacovazzi, B.; Kim, D.; et al. The Global Space-Based Inter-Calibration System (GSICS). *Bull. Am. Meteorol. Soc.* **2011**, *92*, 467–475. [CrossRef]
2. Wielicki, B.A.; Young, D.F.; Mlynczak, M.G.; Thome, K.J.; Leroy, S.; Corliss, J.; Anderson, J.G.; Ao, C.O.; Bantges, R.; Best, F.; et al. Achieving climate change absolute accuracy in orbit. *Bull. Am. Meteorol. Soc.* **2013**, *94*, 1519–1539. [CrossRef]

3.　Tobin, D.; Holz, R.; Nagle, F.; Revercomb, H. Characterization of the Climate Absolute Radiance and Refractivity Observatory (CLARREO) ability to serve as an infrared satellite intercalibration reference. *J. Geophys. Res. Atmos.* **2016**, *121*, 4258–4271. [CrossRef]

4.　Thorne, P.W.; Lanzante, J.R.; Peterson, T.C.; Seidel, D.J.; Shine, K.P. Tropospheric temperature trends: History of an ongoing controversy. *Wiley Interdiscip. Rev. Clim. Chang.* **2011**, *2*, 66–88. [CrossRef]

5.　Grody, N.C.; Vinnikov, K.Y.; Goldberg, M.D.; Sullivan, J.T.; Tarpley, J.D. Calibration of multisatellite observations for climatic studies: Microwave Sounding Unit (MSU). *J. Geophys. Res.* **2004**, *109*, D24104. [CrossRef]

6.　Bodeker, G.E.; Bojinski, S.; Cimini, D.; Dirksen, R.J.; Haeffelin, M.; Hannigan, J.W.; Hurst, D.F.; Leblanc, T.; Madonna, F.; Maturilli, M.; et al. Reference upper-air observations for climate: From concept to reality. *Bull. Am. Meteorol. Soc.* **2015**, *97*, 123–135. [CrossRef]

7.　Kroodsma, R.A.; McKague, D.S.; Ruf, C.S. Vicarious cold calibration for conical scanning microwave imagers. *IEEE Trans. Geosci. Remote Sens.* **2017**, *55*, 816–827. [CrossRef]

8.　Yang, H.; Zhou, J.; Weng, F.; Sun, N.; Anderson, K.; Liu, Q.; Kim, E.J. Developing vicarious calibration for microwave sounding instruments by using lunar radiation. *IEEE Trans. Geosci. Remote Sens.* **2018**, *56*, 6723–6733. [CrossRef]

9.　Houtz, D.A.; Emery, W.; Gu, D.; Jacob, K.; Murk, A.; Walker, D.K.; Wylde, R.J. Electromagnetic design and performance of a conical microwave blackbody target for radiometer calibration. *IEEE Trans. Geosci. Remote Sens.* **2017**, *55*, 4586–4596. [CrossRef]

10.　Rosenkranz, P.W.; Blackwell, W.J.; Gasiewski, A.J.; Leslie, R.V.; Mears, C.A.; Piepmeier, J.R.; Racette, P. E.; Santer, B.D. Designing a Climate-Monitoring Microwave Radiometer. In Proceedings of the USNC-URSI National Radio Science Meeting, Boulder, CO, USA, 4–7 January 2017. [CrossRef]

11.　Blackwell, W.J.; Bishop, R.; Cahoy, K.; Cohen, B.; Crail, C.; Cucurull, L.; Dave, P.; DiLiberto, M.; Erickson, N.; Fish, C.; et al. Radiometer calibration using colocated GPS radio occultation measurements. *IEEE Trans. Geosci. Remote Sens.* **2014**, *52*, 6423–6433. [CrossRef]

12.　Draper, D.W.; Newell, D.A.; McKague, D.S.; Piepmeier, J.R. Assessing Calibration Stability Using the Global Precipitation Measurement (GPM) Microwave Imager (GMI) Noise Diodes. *IEEE J. Sel. Top. Appl. Earth Obs. Remote Sens.* **2015**, *8*, 4239–4247. [CrossRef]

13.　Ochiai, S.; Kikuchi, K.; Nishibori, T.; Manabe, T. Gain nonlinearity calibration of submillimeter radiometer for JEM/SMILES. *IEEE J. Sel. Top. Earth Obs. Remote Sens.* **2012**, *5*, 962–969. [CrossRef]

14.　Piepmeier, J.R.; Gasiewski, A.J. Digital correlation microwave polarimetry: Analysis and demonstration. *IEEE Trans. Geosci. Remote Sens.* **2001**, *39*, 2392–2410. [CrossRef]

15.　Yagoubov, P.; Murk, A.; Wylde, R.; Bell, G.; Tan, G.H. Calibration loads for ALMA. In Proceedings of the 36th International Conference on Infrared, Millimeter, and Terahertz Waves, Houston, TX, USA, 2–7 October 2011. [CrossRef]

16.　Liu, C.-Y.; Li, J.; Ho, S.-P.; Liu, G.-R.; Lin, T.-H.; Young, C.-C. Retrieval of atmospheric thermodynamic state from synergistic use of radio occultation and hyperspectral infrared radiances observations. *IEEE J. Sel. Top. Earth Obs. Remote Sens.* **2016**, *9*, 744–756. [CrossRef]

17.　CoSMIR. Available online: https://atmospheres.gsfc.nasa.gov/meso/index.php?section=121 (accessed on 1 November 2019).

18.　Kursinski, E.R.; Hajj, G.A.; Leroy, S.S.; Hermann, B. The GPS radio occultation technique. *Terr. Atmos. Ocean. Sci.* **2000**, *11*, 53–114. [CrossRef]

19.　Kursinski, E.R.; Hajj, G.A.; Schofield, J.T.; Linfield, R.P.; Hardy, K.R. Observing Earth's atmosphere with radio occultation measurements using the Global Positioning System. *J. Geophys. Res.* **1997**, *102*, 23429–23465. [CrossRef]

20.　Foelsche, U.; Scherllin-Pirscher, B.; Ladstädter, F.; Steiner, A.K.; Kirchengast, G. Refractivity and temperature climate records from multiple radio occultation satellites consistent within 0.05%. *Atmos. Meas. Tech.* **2011**, *4*, 2007–2018. [CrossRef]

21.　Cimini, D.; Rosenkranz, P.W.; Tretyakov, M.Y.; Koshelev, M.A.; Romano, F. Uncertainty of atmospheric microwave absorption model: Impact on ground-based radiometer simulations and retrievals. *Atmos. Chem. Phys.* **2018**, *18*, 15231–15259. [CrossRef]

22. Rüeger, J.M. Refractive index formulae for radio waves. In Proceedings of the FIG XXII International Congress, Washington, DC, USA, 19–26 April 2002. Available online: http://www.fig.net/resources/proceedings/fig_proceedings/fig_2002/Js28/JS28_rueger.pdf (accessed on 1 November 2019).

23. Leroy, S.; Ao, C.O.; Verkhoglyadova, O.P. Temperature trends and anomalies in modern satellite data: Infrared sounding and GPS radio occultation. *J. Geophys. Res. Atmos.* **2018**, *123*, 11431–11444. [CrossRef]

24. Khaykin, S.M.; Funatsu, B.M.; Hauchecorne, A.; Godin-Beekmann, S.; Claud, C.; Keckhut, P.; Pazmino, A.; Gleisner, H.; Nielsen, J.K.; Syndergaard, S.; et al. Postmillennium changes in stratospheric temperature consistently resolved by GPS radio occultation and AMSU observations. *Geophys. Res. Lett.* **2017**, *44*, 7510-–7518. [CrossRef]

25. Leroy, S. Anderson, J.G.; Ohring, G. Climate signal detection times and constraints on climate benchmark accuracy requirements. *J. Clim.* **2008**, *21*, 841–846. [CrossRef]

26. Mears, C.A.; Wentz, F.J.; Thorne, P.; Bernie, D. Assessing uncertainty in estimates of atmospheric temperature changes from MSU and AMSU using a Monte-Carlo estimation technique. *J. Geophys. Res.* **2011**, *116*, D08112. [CrossRef]

27. Mears, C.A.; Wentz, F.J. Sensitivity of satellite-derived tropospheric temperature trends to the diurnal cycle adjustment. *J. Clim.* **2016**, *29*, 3629–3646. [CrossRef]

28. Mears, C.A.; Wentz, F.J. A satellite-derived lower-tropospheric atmospheric temperature dataset using an optimized adjustment for diurnal effects. *J. Clim.* **2017**, *30*, 7695–7718. [CrossRef]

29. Wentz, F.J.; Schabel, M. Effects of orbital decay on satellite-derived lower-tropospheric temperature trends. *Nature* **1998**, *394*, 661–664. [CrossRef]